J|A|C|S
COMMUNICATIONS

Published on Web 09/17/2005

The α-Helix Folds More Rapidly at the C-Terminus Than at the N-Terminus

Angela Pozo Ramajo,[†] Sarah A. Petty,[†,‡] Agnieszka Starzyk,[‡] Sean M. Decatur,[‡] and Martin Volk*,[†]

Department of Chemistry and Surface Science Research Centre, University of Liverpool, Liverpool L69 3BX, U.K., and Department of Chemistry, Mount Holyoke College, South Hadley, Massachusetts 01075

Received July 7, 2005; E-mail: m.volk@liv.ac.uk

We report results of nanosecond temperature jump experiments on a series of α-helical model peptides. The helix-coil dynamics of different peptide sections were observed separately, using isotopic labeling and IR detection in the amide I′ band.[1] The results show that the helix-coil dynamics of the α-helical C-terminus are faster than those of the N-terminus.

The first phase of protein folding is believed to be the formation of secondary structural elements, which then may act as nucleation sites for the formation of native structure. Thus, the dynamics of secondary structure formation is of utmost importance for protein folding. The folding/unfolding transition of α-helical peptides has been reported to occur on the 100-ns time scale,[2−6] mostly from experiments using fast temperature jumps. The rise in temperature disturbs the helix-coil equilibrium of the peptide, and the ensuing helix-coil relaxation can be observed by a suitable technique, such as nanosecond time-resolved IR spectroscopy of the amide I band near 1650 cm^{-1}, which is highly sensitive to secondary structure.[7]

Conventional IR spectroscopy is limited to the determination of *overall* secondary structural content and does not allow the distinction between different structures at the residue level. However, IR spectroscopy can be made site-specific by isotopic labeling of specific residue carbonyls with ^{13}C, which shifts the amide I frequency by approximately 40 cm^{-1}. This method has been used previously for observing helix-coil stability[8,9] and dynamics[3,4] at the residue level. Here, we report measurements on the following series of labeled peptides (underlined residues are ^{13}C-labeled):

4A	AAAAKAAAAKAAAAKAAAAY-NH_2
4AL1	<u>AAAA</u>KAAAAKAAAAKAAAAY-NH_2
4AL2	AAAAK<u>AAAA</u>KAAAAKAAAAY-NH_2
4AL3	AAAAKAAAAK<u>AAAA</u>KAAAAY-NH_2
4AL4	AAAAKAAAAKAAAAK<u>AAAA</u>Y-NH_2

The synthesis, CD spectra, and FTIR analysis of these peptides have been described.[8] Whereas no significant absorbance is found at 1600 cm^{-1} for the unlabeled peptide 4A, FTIR spectra of the labeled peptides show a band near 1600 cm^{-1}, arising from labeled residues in the helical conformation. Its size correlates well with the predicted helix content of the labeled sections, which is significantly lower for 4AL1 and 4AL4 than for 4AL2 and 4AL3, indicating the fraying of the helix at both the N- and C-terminus.

Helix-coil dynamics were observed as described previously.[6] Peptides were dissolved at 20 mg/mL in 0.1% phosphoric acid/D_2O and placed in a temperature-controlled IR cell (50 μm spacer). A Nd:YAG/dye laser system with an IR difference frequency generator provided 3 mJ pump pulses of 7 ns pulse width for direct heating of D_2O at 1970 nm, yielding temperature jumps of 5 °C.[10] Time-resolved IR absorbance changes at 1601 cm^{-1} (amide I′ frequency of ^{13}C-labeled residues in helical conformation) and 1632 cm^{-1} (unlabeled helical peptide) were monitored using an IR laser diode and a 50-MHz detector (signal rise time, 14 ns).

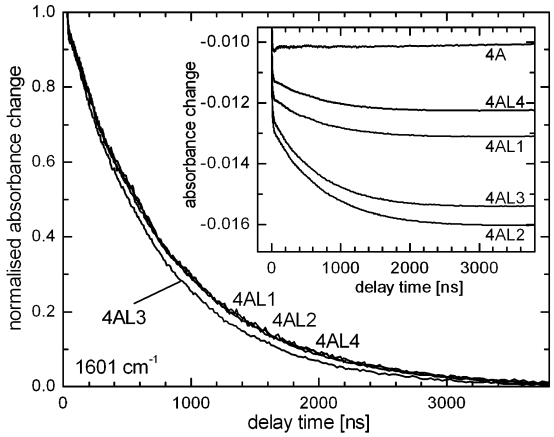

Figure 1. Time-dependent absorbance changes at 1601 cm^{-1} for the labeled peptides 4AL1, 4AL2, 4AL3, and 4AL4 after temperature jumps from 4 to 9 °C, normalized to the amplitude of the dynamic component on the 100-ns time scale. Inset: Absorbance changes at 1601 cm^{-1} for the unlabeled peptide 4A and the labeled peptides, not normalized.

Table 1. Segmental Helix-Coil Relaxation Time Constants, τ_{rel}, and Amplitude of the Absorbance Changes, ΔA, Measured in the Labeled Peptides at 1601 cm^{-1}[a]

	4°C → 9°C		11°C → 16°C	
peptide	τ_{rel}/ns	ΔA	τ_{rel}/ns	ΔA
4AL1	814 ± 9	0.0015	382 ± 6	0.0011
4AL2	801 ± 10	0.0035	376 ± 5	0.0027
4AL3	730 ± 6	0.0032	349 ± 3	0.0022
4AL4	818 ± 22	0.0014	373 ± 9	0.0009
4A[b]	806 ± 6	0.0077	367 ± 5	0.0062

[a] For comparison, the overall helix-coil relaxation time constant, measured in the unlabeled peptide 4A at 1632 cm^{-1}, is included. [b] Overall helix-coil relaxation time constant, measured at 1632 cm^{-1}.

Figure 1 shows temperature-jump-induced absorbance changes. The absorbance of D_2O at 1601 cm^{-1} decreases with increasing temperature, which is responsible for the major part of the instantaneous bleaching; a smaller instantaneous bleach arises from a temperature-induced shift of the helical amide I′ frequency.[2,4] For the unlabeled peptide 4A, no further absorbance changes were observed at 1601 cm^{-1} on the nanosecond time scale (see Figure 1), although the absorbance at 1632 cm^{-1} decreases upon helix melting on the 100-ns time scale, as expected (Table 1). For the labeled peptides, the absorbance at 1601 cm^{-1} decreases on this time scale due to the melting of helical structures in the labeled peptide sections. In agreement with the previous FTIR results on these peptides,[8] the amplitude of these absorbance changes is smaller for the peptides labeled at the ends than for those labeled in the center (see Figure 1), due to the lower helix content of the peptide

[†] University of Liverpool.
[‡] Mount Holyoke College.

10.1021/ja054500+ CCC: $30.25

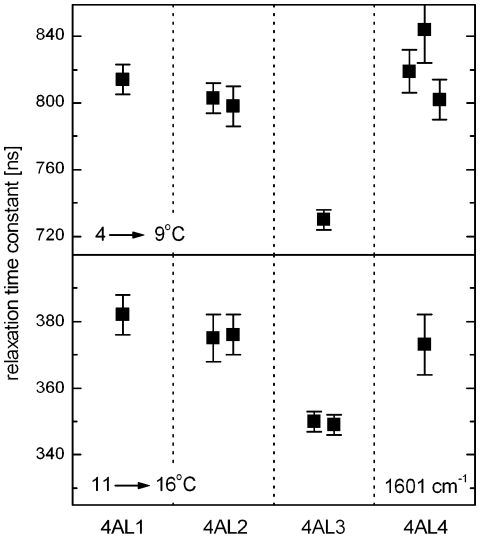

Figure 2. Segmental helix-coil relaxation time constants measured at 1601 cm^{-1} for isotopically labeled peptides after temperature jumps from 4 to 9 °C and from 11 to 16 °C, respectively. Multiple results for the same peptide result from repeat measurements with fresh samples.

ends. The segmental helix-coil relaxation times, obtained from single-exponential fits[11] of the data for temperature jumps from 4 to 9 °C and from 11 to 16 °C, are summarized in Table 1 and Figure 2. In all cases, the data were found to be well described by a single-exponential function.

It can be clearly seen in Figure 1 and from the fit results that the third peptide section has the fastest helix-coil relaxation. In particular, it is faster than that of the second section, although these two sections are identical in amino acid content and sequence, have the same neighboring residues, and have highly similar helix content.[8] Previous dynamic measurements on an α-helical peptide isotopically labeled in its three alanine-containing sections showed different dynamics for the section adjacent to the peptide's helix-stabilizing N-terminal sequence, the middle section, and the section adjacent to its C-capping group.[4] Here, on the other hand, we report differences in dynamics even among central sections with identical composition and neighboring residues.[12] We ascribe this observation to different dynamics of the C- and N-terminal *helix* ends.

It is well known that alanine-based peptides form only marginally stable helices and are in a dynamic equilibrium between different structures containing helical *and* disordered peptide segments. Most of the helical structures extend over the center of the peptide, whereas the ends are frayed.[8] With an overall helicity of 50−60%,[8] there is a significant probability for helices to start in the second section and/or end in the third one. Using parameters that yield overall helicities around 50%, the single-chain Zimm−Bragg model[13] predicts the C-terminal helix end to occur at least four times as often in the third section than in the second section, whereas the opposite is true for the N-terminal helix end. Since the formation of multiple helical segments in short peptides is entropically disfavored, helical structures decrease in length by "unraveling" from their ends. Thus, the segmental helix-coil relaxation times observed for the second and third peptide sections are dominated by the helix-coil relaxation of the helical N- and C-terminal ends, respectively, and our results show that the helix-coil dynamics of the C-terminal helix end is faster than that of the N-terminal end.

The two ends of an α-helix are not structurally equivalent.[14] The backbone carbonyls of the last three residues with helical conformation at the C-terminal end of the helix are not hydrogen bonded, which results in reduced steric restrictions and a wider conformational distribution of the final helical residues.[15] Moreover, they are less protected from solvent access by side chains than those at the helical N-terminus. Most likely, the faster helix-coil dynamics at the C-terminal helix end observed here result from these effects which may lead to a lower activation barrier for intrapeptide hydrogen bond formation.

Although faster helix folding and unfolding at the C-terminal end has been predicted by molecular dynamics simulations,[16] the results reported here are the first experimental verification of this effect. They show that helix propagation is direction dependent; i.e., an α-helix, once nucleated, grows more rapidly toward the peptide's C-terminus than toward the N-terminus. Any complete description of the dynamics of α-helix folding must take this asymmetry into account, which could be an important aspect of kinetically controlling the correct folding of protein sections.

In summary, we have shown that time-resolved IR spectroscopy in combination with isotopic labeling can be used to obtain helix-coil dynamics at the residue level. Our results show that the folding of an α-helix proceeds more rapidly at the helical C-terminus than at the N-terminus, presumably because of reduced steric restrictions due to the non-hydrogen-bonded carbonyl groups.

Acknowledgment. Financial support from the EPSRC, the University of Liverpool, the NSF (RUI 0415878), and the Dreyfus Foundation is gratefully acknowledged. We are most grateful for a laser loan from the CCLRC Central Laser Facility.

References

(1) The prime indicates deuterated amides.
(2) Williams, S.; Causgrove, T. P.; Gilmanshin, R.; Fang, K. S.; Callender, R. H.; Woodruff, W. H.; Dyer, R. B. *Biochemistry* **1996**, *35*, 691.
(3) Werner, J. H.; Dyer, R. B.; Fesinmeyer, R. M.; Andersen, N. H. *J. Phys. Chem. B* **2002**, *106*, 487.
(4) (a) Huang, C.-Y.; Getahun, Z.; Wang, T.; DeGrado, W. F.; Gai, F. *J. Am. Chem. Soc.* **2001**, *123*, 12111. (b) Huang, C.-Y.; Getahun, Z.; Zhu, Y.; Klemke, J. W.; DeGrado, W. F.; Gai, F. *Proc. Natl. Acad. Sci. U.S.A.* **2002**, *99*, 2788.
(5) (a) Thompson, P. A.; Eaton, W. A.; Hofrichter, J. *Biochemistry* **1997**, *36*, 9200. (b) Petty, S. A.; Volk, M. *Phys. Chem. Chem. Phys.* **2004**, *6*, 1022. (c) Bredenbeck, J.; Helbing, J.; Kumita, J. R.; Woolley, G. A.; Hamm, P. *Proc. Natl. Acad. Sci. U.S.A.* **2005**, *102*, 2379.
(6) Pozo Ramajo, A.; Petty, S. A.; Volk, M. *Chem. Phys.*, in press.
(7) Krimm, S.; Bandekar, J. *Adv. Protein Chem.* **1986**, *38*, 181.
(8) Decatur, S. M. *Biopolymers* **2000**, *54*, 180.
(9) (a) Decatur, S. M.; Antonic, J. *J. Am. Chem. Soc.* **1999**, *121*, 11914. (b) Venyaminov, S. Y.; Hedstrom, J. F.; Prendergast, F. G. *Proteins: Struct., Funct. Genet.* **2001**, *45*, 81.
(10) The temperature jump size was measured using the temperature-dependent absorbance change of D_2O at 1570 cm^{-1}, where no peptide absorbance is found, and calibrated by temperature-dependent FTIR spectra.
(11) For the determination of relaxation time constants, data were corrected for the onset of cooling, which is indicated by a slight recovery of the D_2O absorbance bleach at 1570 cm^{-1} (~1% within 3 μs, compare the 4A data at 1601 cm^{-1}, Figure 1) by dividing by $[0.95 + 0.05 \exp(-t/10000)]$, where t denotes the delay time (in ns), which well describes the D_2O absorbance recovery at 1570 cm^{-1} (see ref 6). The corrected data after 60 ns were then fitted to a single exponential using nonlinear least-squares fitting. For each peptide, at least 25 600 single measurements were taken and analyzed in groups of 2560; time constants and their errors in Table 1 and Figure 2 are the average and standard deviation of the results of these separate fits. We have found that this method yields realistic error estimates, with repeat measurements reproducing results within the error bars (compare Figure 2 and ref 6).
(12) We restrict our discussion to the middle sections, since the outer sections will be affected by the previously reported capping group effects.
(13) Zimm, B. H.; Bragg, J. K. *J. Chem. Phys.* **1959**, *31*, 526.
(14) (a) Aurora, R.; Rose, G. D. *Protein Sci.* **1998**, *7*, 21. (b) Penel, S.; Hughes, E.; Doig, A. J. *J. Mol. Biol.* **1999**, *287*, 127.
(15) Ho, B. K.; Thomas, A.; Brasseur, R. *Protein Sci.* **2003**, *12*, 2508.
(16) (a) Sung, S. S. *Biophys. J.* **1994**, *66*, 1796. (b) Voegler Smith, A.; Hall, C. K. *Proteins: Struct., Funct. Genet.* **2001**, *44*, 344.

JA054500+